MICROSTRUCTURE AND PROPERTIES OF DIAMOND CUTTING EDGES IMPROVED BY NANOMATERIALS IN TOOL POLISHING

Bo Wang[1], Liping Huang[1], Qijing Zhang[2]*
[1]College of Intelligent Manufacturing, Yangzhou Polytechnic Institute, Yangzhou, 225127, China
[2]Department of Basic Science, Yangzhou Polytechnic Institute, Yangzhou, 225127, China

Abstract - This study aims to solve the polishing problems caused by the excessive hardness difference between nano-polycrystalline diamond tool materials and tip support materials, and improve the polishing quality and processing accuracy of nano-polycrystalline diamond cutting edges. In this study, nano-reinforced tip support materials are prepared by introducing nano-alumina particles and graphene nanosheets into silver-copper-titanium-based support materials. The influence of laws of different nanomaterial contents and polishing process parameters on the microstructure and properties of cutting edges is systematically explored. Experimental results show that when the content of nano-alumina particles is 1.25%, the hardness of the support material reaches the maximum value of 1.42 gigapascals. When the content of graphene nanosheets is 0.2%, the peak hardness of the support material is 1.37 gigapascals. Both nanomaterials can improve the hardness and impact resistance of the support material through dispersion strengthening and interface shear effects. After polishing assisted by the enhanced support material, the interface height difference between the nano-polycrystalline diamond tool and the support material is reduced from 50.2 nanometers to 22.2 nanometers. The cutting-edge bluntness radius is decreased from 57 nanometers to 42 nanometers, which effectively improves the vibration and noise problems during the polishing process. The polishing process parameters are optimized through single-factor variable experiments, and the optimal combination is determined as follows: The rotation speed of the polishing machine is 1,600 rpm; The diamond abrasive particle size is 0.25 microns; The polishing pressure is 2.6 Newtons. Under these conditions, the minimum surface roughness of the nano-polycrystalline diamond tool can reach 0.44 nanometers, and the minimum cutting edge bluntness radius is 40.11 nanometers, which fully meets the requirements of high-precision machining for tool surface quality. Through the dual means of nanomaterial modification and process parameter optimization, this study provides a new solution to solve the material matching problem in the polishing process of nano-polycrystalline diamond tools. This paper has important engineering application value for promoting the development of high-precision diamond cutting technology and the innovative design of support materials.

Keywords: Nano-polycrystalline diamond; Cutting-edge support material; Nanomaterials; Polishing process parameters; Microstructure; Surface roughness; Cutting performance.

1. Introduction

The continuous development of modern manufacturing technology has led to increasingly high requirements for tool performance. Among them, Nano-polycrystalline Diamond (NPD) cutting tools are widely used in industrial manufacturing and are commonly used in high-precision manufacturing processes [1]. NPD, as a high-performance diamond cutting tool material, has high strength, hardness, and wear resistance, and it maintains high strength stability even in complex working environments [2-3]. For example, in experimental environments, NPD cutting tools can maintain a hardness of over 800 GPa at 100 ℃, making them widely used in high-temperature machining scenarios such as ceramics and aluminum alloys [4]. However, although NPD cutting tools have demonstrated excellent mechanical properties and stability, they face many problems in polishing environments [5]. Due to the high-strength performance characteristics of NPD materials, it is difficult for NPD tools to obtain effective Cutting-Edge Support Materials (CESMs), and the huge hardness difference between CESMs and NPD

© 2026. The Author(s). Published by Cefin Publishing House – Bucharest, https://ijomam.com/

Copyright: © 2026 by the authors. Licensee IJOMAM, Romania. This article is an open access article distributed under the terms and conditions of the Creative Commons. Attribution (CC BY) license (https://creativecommons.org/licenses/by/4.0/)
dx.doi.org/10.17683/ijomam/issue24.5

materials poses challenges for polishing the cutting-edge structure of NPD tools [6-7]. At present, Nano-Alumina Particles (NAPs) and Graphene Nanosheets (GNS) are considered to effectively improve the hardness of CESMs due to their excellent physical and chemical properties [8]. Among them, NAP has advantages such as a high melting point, high hardness, good chemical stability, and electrical insulation. According to relevant research, the nanoscale effect results in a larger specific surface area and stronger adsorption capacity, which can significantly improve the strength and toughness of materials [9-10]. In addition, GNS materials have high-strength mechanical and thermal properties and are widely used in the fields of medicine, aerospace, and composite materials. In the CESM of NPD cutting tools, studies have found that GNS can significantly improve the toughness and impact resistance of the tool, effectively reducing the risk of tool chipping and fracture during cutting [11].

In addition, polishing NPD cutting tools is a key step in improving their cutting-edge quality and performance. The main purpose of polishing is to reduce surface roughness, remove damaged layers, and ultimately obtain a smooth and undamaged cutting-edge tissue surface. The polishing effect of NPD cutting tools will directly affect the machining accuracy and service life of the tools, and have a direct impact on the flatness and sharpness of the tools. NPD cutting tools are mainly affected by factors such as mechanical polishing speed, polishing pressure, and abrasive particle size during polishing [12]. Related studies have shown that appropriate rotational speed can create a stable flow field for polishing solution and abrasive particles on the polishing disc, thereby better removing small defects on the tool surface [13]. The polishing pressure will affect the contact effect between the abrasive particles and the material surface. Excessive pressure can wear down the cutting surface and cause damage to the cutting-edge structure of the tool. Diamond Abrasive Particle Size (DAPS) is mainly used to remove small undulating particles on the surface of cutting tools. A particle size that is too small can affect the efficiency of impurity removal during material polishing, while a particle size that is too large can damage the cutting-edge structure of the tool and leave deep scratches [14].

In summary, existing literature has fully confirmed the excellent performance of NPD tools, the enhancement effect of nanomaterials on support materials, and the impact of polishing parameters on surface integrity. However, there is a lack of systematic solutions integrating "nanomaterial modification + process parameter collaborative optimization" targeting the core pain point of hardness mismatch between NPD materials and support materials. Most of the existing research focuses on single-variable optimization and lacks in-depth exploration of multi-factor coupling effects. This is the research gap that this study aims to fill.

This study has two innovations. One is to introduce GNS and NAP into the CESM of NPD tools, which improves the hardness of the supporting material, reduces the noise and vibration during the polishing process, and provides a machining foundation for subsequent tool polishing. Second, by controlling the processing condition parameters and analyzing different processing pressures, processing speeds, and abrasive particle sizes, the optimal processing conditions for NPD tools are obtained, and the processing efficiency of the tools is improved. This study effectively solves the problem of material hardness mismatch in NPD tool polishing through collaborative innovation of nano-modified support materials and optimization of polishing process parameters, and significantly improves the accuracy of edge processing. This paper provides practical and reliable technical solutions for the engineering application of high-precision diamond cutting technology and promotes the incremental upgrade of technology in this field.

2. Methods and Materials

2.1 Experimental Materials and Equipment

Experimental material: NPD block, provided by Sumitomo Electric of Japan; Silver (Ag), with purity of 99.99%, provided by Ningbo Guangxin Nanomaterials; Copper (Cu),with a 4N copper powder with a purity of 99.99%, provided by Ningbo Zhengyuan Copper Alloy Co., Ltd; Titanium (Ti), with a purity of 99.99%, provided by STAINLESS company; GNS, provided by Jiangsu Xianfeng Nanomaterials Technology Co., Ltd; Dilute nitric acid solution (HNO3), with a concentration of 10%, provided by Beijing Beina Chuanglian Biotechnology; Hydrogen peroxide solution (H2O2), with analytical grade, provided by Yonghua Chemical.

Experimental setup: Vacuum welding machine, UNITEMP RSO-200, provided by UNITEMP; Press in Vickers hardness tester, Fness V02625CA, provided by Suzhou Fermat Automation Technology Co., Ltd; Hopkinson pressure bar, ZDSHPB-20, provided by Shandong Zongde Electromechanical Equipment Co., Ltd; Flat polishing machine, X600, provided by Shanghai Guangxiang Sample Preparation Equipment Co., Ltd; Circular blade polishing machine, YTYP-1200, provided by Foshan Yongtao Electromechanical Equipment; Scanning Electron Microscope (SEM), JSM-IT210, provided by Japan Electronics Corporation; The stylus roughness measurement profilometer, SJ5800, provided by Shenzhen Zhongtu Instrument.

2.2 Preparation of NPD Tool Reinforcement Material

2.2.1 Screening of Reinforcement Materials

There is a significant difference in hardness between the NPD tool and its CESM, resulting in a significant nanometer height difference between the NPD tool and its tip holder. This directly affects the protective effect of the tip bracket on the tool and affects the subsequent polishing process of the NPD tool. If the height difference is large, NPD tools will produce high noise and continuous vibration during the polishing process [15-16]. Even if the impact can be reduced by controlling the speed of the polishing turntable, it will still affect the actual polishing effect of NPD tools. To address this, increasing the hardness of CESE itself and reducing the difference in hardness between it and NPD materials can effectively remove excess cutting edge material and reduce height differences through polishing. In this regard, this study attempts to increase the use of nanomaterials to improve the performance of CESM. At present, GNS and nano-aluminum particles have shown excellent performance in metal alloy improvement. Related studies have shown that it can enhance the hardness of cutting-edge support.

Especially when 20 nm alumina material particles are added, which can improve the surface smoothness of the cutting tool. However, there are still many micro pits and unstable bonding between NPD and supporting materials. According to relevant research, the addition of GNS can effectively remove the surface of CESM. Therefore, this study uses GNS and alumina particles to improve cutting-edge support.

2.2.2 Preparation of Reinforcement Materials

The study selects Ag Cu Ti as the basic support composite material. The proportions of Cu, Ag, and Ti selected are 19.65%, 43.56%, and 2.91%, respectively. A total of 2,000 g of mixed materials is placed in a drying oven, and then the temperature is raised by 200 ℃ until dry, and then cooled to room temperature for shaping. Next, the dried mixture is sent into a vacuum welding machine, and the temperature is increased to 800 ℃ for 10 minutes.

Table 1. Material ratio of reinforced part of CESM

Number	Mass ratio of NAPs (%)	Mass of NAPs (g)	Mass ratio of GNS (%)	Mass of GNS (g)	CESM raw material quality (g)
1	0.5	0.00400	0.2	0.00160	0.811
2	1.0	0.00809	0.2	0.00160	0.811
3	1.25	0.01008	0.2	0.00160	0.811
4	1.50	0.12149	0.2	0.00160	0.811
5	2.0	0.01518	0.2	0.00160	0.811
6	1.0	0.00820	0.1	0.00079	0.811
7	1.0	0.00820	0.2	0.00159	0.811
8	1.0	0.00820	0.3	0.00244	0.811
9	1.0	0.00820	0.4	0.00325	0.811
10	0.0	0	0	0	0.811

Next, the mixed Ag-Cu-T material is subjected to a cooling operation until it becomes liquid, and different proportions of GNS and alumina particles are added to fully encapsulate the nanoparticles in the liquid. Table 1 shows the ratio of reinforcement materials.

After the material is fully cooled and solidified into a solid, the base material is then placed in metal processing equipment for basic treatment.

The basic material is processed into a cylindrical material with a height of 4 mm and a diameter of 2 mm, and its surface is machine-polished by a material polishing machine.

2.3 Polishing of NPD Tool Cutting Edge Structure

2.3.1 Scheme Analysis

NPD cutting tools and workpiece materials are usually in point contact, which can better meet the mechanical requirements for precision machining of cutting tools. In the experiment, NPD cutting tools are processed using a curved edge geometry profile, with the front and rear cutting surfaces being flat and circular arc surfaces. The cross-section of the cutting edge of the NPD tool is shown in Figure 1.

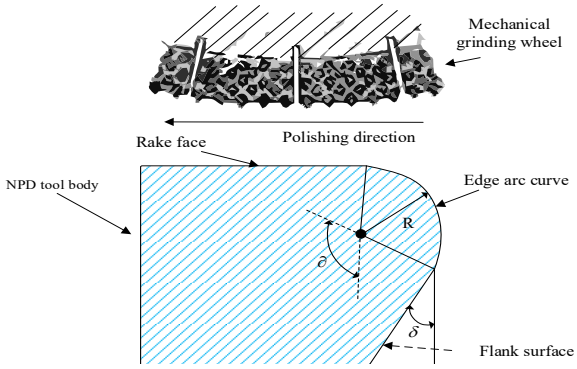

Figure 1: Cross-sectional model of NPD tool cutting edge

To ensure that NPD cutting tools have sufficient sharpness, it is necessary to enhance the quality of their front and rear cutting surfaces to improve the overall performance of the tools. In addition, the bluntness radius of the cutting edge is a key parameter for tool precision, which directly affects its machining effect in the field of more precise materials [17]. Therefore, to ensure the performance of NPD cutting tools, different polishing conditions will be used to process the cutting edge tissue interface, and the polishing effect of the cutting edge tissue will be evaluated by surface roughness and bluntness radius. The calculation of roughness Sa is shown in equation (1) [18].

$$Sa = \frac{1}{A}\int\int_{A}|z(x,y)|\,dxdy \tag{1}$$

In equation (1), A is the total surface area. $z(x,y)$ is the height deviation of point (x,y) on the surface relative to the average plane. The smaller the Sa value, the smoother the tool surface, and the larger the Sa value, the rougher it is, measured in nm.

Measurement of tool bluntness radius: The NPD tool is fixed on the worktable of the measuring instrument, ensuring that the cutting edge of the tool is perpendicular to the direction of movement of the measuring needle. Then, the instrument starts to move the measuring needle at a constant speed along the cutting edge of the tool. The measuring needle will move up and down with the microscopic undulations of the tool surface contour.

The contour information of the lower tool surface is recorded [19]. Finally, the collected data are processed through the software of the instrument to obtain the blunt radius of the cutting edge of the tool.

2.3.2 Polishing process of cutting edge structure

The pre-prepared NPD block is placed into the vacuum welding machine and connected to the high-speed steel tool handle to obtain the blank of the tool to be processed. Then, the circular arc blade polishing machine is used to polish the blade surface. The grinding wheel speed is set to 6,000 rpm, the grinding wheel diameter is 90 mm, and the polishing force is 6 N. Polishing requires a tool rake angle of 10° and a tool surface roughness of 1 nm. Then, the reinforcement material prepared in Section 2.2 is coated on the tool surface after NPD and heated to 800 °C in a vacuum welding machine for 15 minutes for sintering treatment, so that the composite material is completely dissolved. Subsequently, GNS and alumina particles are placed in it and wrapped in the composite material solution, waiting for cooling to solidify on the back cutting surface.

After completing the above steps, a flat polishing machine is used to process the cutting edge structure, mechanically polishing until there is no harsh noise or vibration. Finally, the prepared HNO3 and H2O2 solutions are used to treat the CESM to obtain sharp knives. The entire NPD tool polishing process is shown in Figure 2.

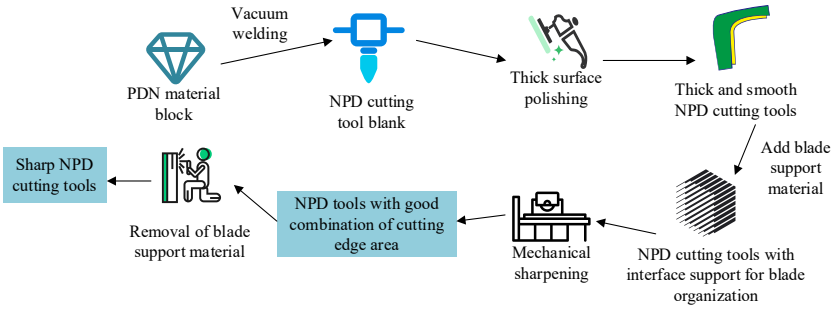

Figure 2: NPD tool polishing process flow

3. Results and Discussion

3.1 Material Hardness Testing

Before polishing NPD cutting tools, it is necessary to ensure that the height difference between the polishing surface and its cutting edge support is minimized to ensure the effectiveness of the NPD blade. Therefore, this study uses two types of nanomaterials, GNS and NAP, to improve the cutting-edge support, and conducted hardness testing on both materials using a Vickers hardness tester (with a device load of 100 g). Figure 3 (a) shows the effect of different alumina contents on hardness.

The NAP content increases from 0% to 1.25%, and the hardness of the material shows an increasing region. Then, as the NAP content continues to increase, the hardness decreases from the highest hardness of 1.42 GPa at 1.25% NAP to 1.15 GPa at 2.0% NAP. Next, the effect of GNS on hardness is tested, as shown in Figure 3 (b). Similarly, the hardness value of GNS increases in the range of 0% to 0.2% content, and then continues to increase, resulting in a decrease in hardness value.

The maximum hardness value of 0.2% GNS is 1.37 GPa. A comprehensive comparison is made between the effects of two materials on cutting-edge support, with NAP having a greater impact on material hardness.

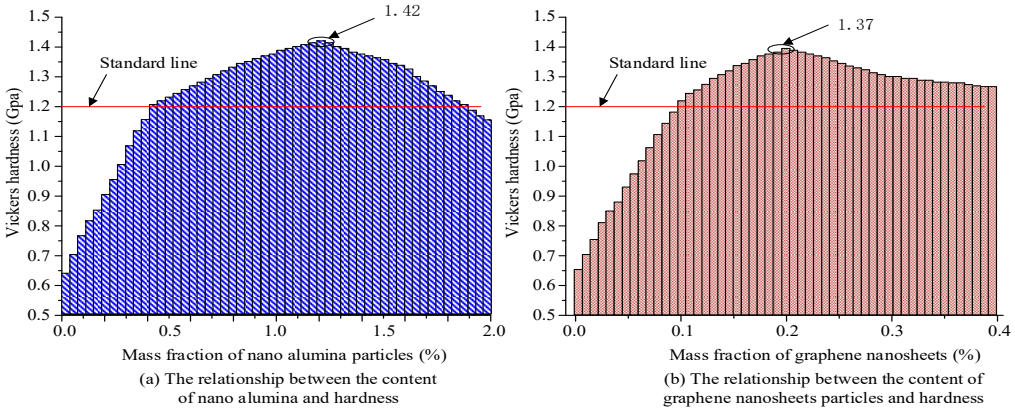

Figure 3: Effects of different NAP and GNS on the hardness of supporting materials

3.2 Impact Resistance Experiment of Cutting-edge Support

The impact resistance test can reflect whether the supporting material has a good protective effect on the cutting edge of the tool. Therefore, the impact experiment is conducted using a Hopkinson pressure bar, with graphene as GNS.

Figure 4 (a) shows the effect of NAP content on stress. When the content of both materials is 0%, the stress on the supporting material becomes gentle as the strain increases. When keeping the GNS content constant at 2% and continuously adjusting the NAP content, the maximum stress reaches 7.5 GPa with the increase of strain in the experiment when adding aluminum oxide (1.25%). As the stress gradually increases, the material itself has ductility, and adding alumina (0%) can achieve a maximum strain of 3.6 mm. Overall, to maintain the optimal stress of the material, the maximum stress is achieved when the alumina content is 1.25%.

Figure 4 (b) shows the effect of GNS on stress, while keeping the alumina particle content constant at 0.1%. When the GNS content is 0.2%, the maximum material stress is 4.5 GPa. Therefore, the maximum ultimate stress of the material is achieved when the GNS content is 0.2%.

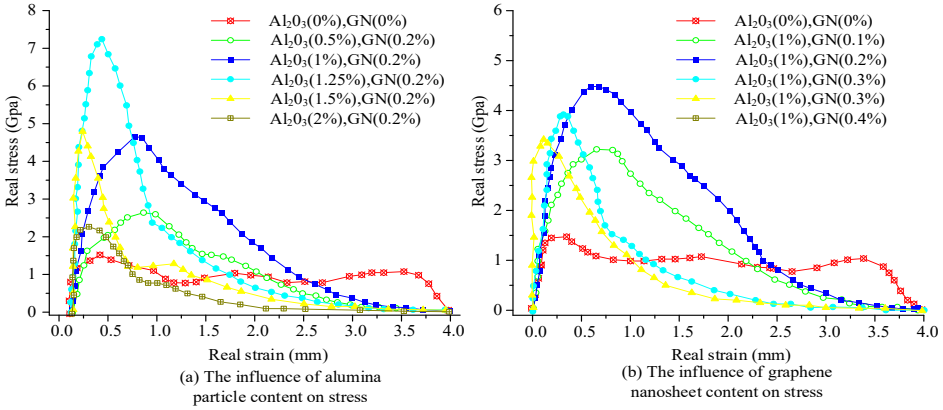

Figure 4: The Effect of different nanomaterial content on cutting edge support stress

Next, this study continues to discuss the failure rate and ultimate strength of materials with different alumina contents. The specific results when GNS is constant at 0.2% are shown in Figure 5 (a). According to the curve, with the increase of alumina content, the failure stress of the supporting material decreases significantly, especially at 1.4%, where the achieved stress is 0.12 mm. In the ultimate strength analysis, the maximum ultimate strength of 7.41 GPa is obtained when the alumina content is 1.25%. Figure 5 (b) shows the failure rate and ultimate strength results at different GNS contents, with a constant alumina content of 1%.

The test results show that GNS can also reduce the failure stress of the supporting material, and when the GNS content reaches 0.4%, the minimum failure stress is 0.15 mm. In the ultimate strength analysis, the maximum ultimate strength of the supporting material is 4.7 GPa at 0.2% GNS. Based on the above analysis, both types of nanomaterials can effectively reduce the failure rate of supporting materials, but it is necessary to maintain the maximum ultimate strength of the materials. Therefore, considering all factors, when the content of GNS and alumina added is 0.2% and 1.25%, the comprehensive performance of the supporting material is the best.

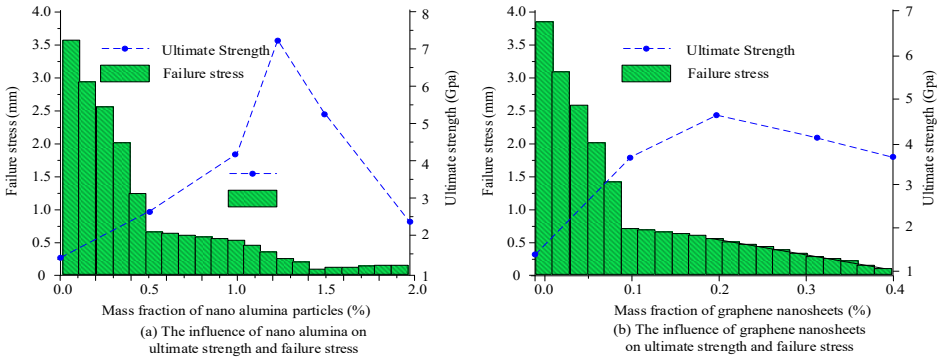

Figure 5: Effect of different nanomaterial content on the failure strain of cutting edge support

3.3 The Influence of Enhancing Cutting Edge Support on NPD Cutting Tools

Next, according to the configuration of GNS (0.2%) and alumina particles (1.25%), they are added to the pre-treated cutting tool CESM (Ag-Cu-Ti complex). Next, this study detects the height difference between the cutting edge and the supporting material surface using an interferometer, and then measures the blunt radius parameter of the cutting edge of the polished tool using a microscope.

Figures 6 (a) and (b) show the polished contour curves of the cutting edge structure under both unreinforced and reinforced support materials. The height difference under the unreinforced support material is 50.2 nm, while the height difference under the reinforced support material is significantly reduced to 22.2 nm after polishing. This indicates that adding two types of nanomaterials can effectively reduce the height difference and strengthen the influence of the support material on the polishing treatment of the cutting edge.

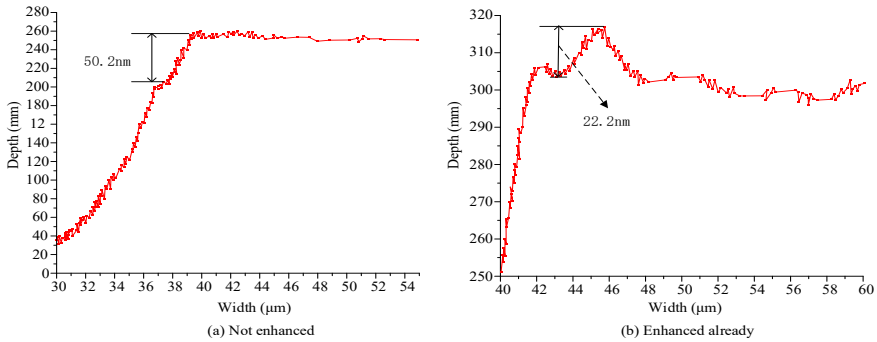

Figure 6: Cutting edge contour curve

Next, this study compares the influence of supporting materials on the bluntness radius of cutting edges. Figures 7 (a) and (b) show the results of the blunt radius of the cutting edge with and without reinforcement of the supporting material.

The enhanced detection results show that the blunt radius of the cutting edge after strengthening the supporting material is 42 nm, which is significantly lower than the unenhanced 57 nm, improving the precision of the NPD tool polishing process.

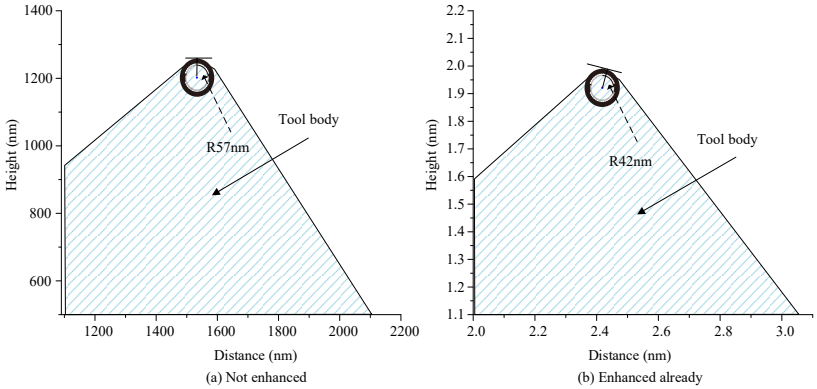

Figure 7: The influence of supporting materials on the bluntness radius of cutting edges

3.4 Influence of Different Rotational Speeds on the Polishing Accuracy of Cutting Tools

Next, in the NPD tool polishing process, multiple variable parameters will be controlled to analyze and obtain the optimal NPD tool polishing parameters. Among them, the polishing effect of the cutting edge of the tool is evaluated by surface roughness and the blunt radius of the cutting edge. The smaller the two values, the higher the polishing accuracy of the cutting edge structure.

Table 2 shows the polishing parameter conditions for NPD cutting tools. DAPS is kept constant at 0.25 μm, while the polishing equipment pressure is kept constant at 2.8 N, and multiple rotational speeds are set to analyze the tool polishing effect.

Table 2. Polishing parameters under changing speed conditions

Parameter number	**1**	**2**	**3**	**4**	**5**	**6**	**7**
Disc polishing speed (RPM)	800	1000	1200	1400	1600	1800	2000
DAPS (μm)	0.25	0.25	0.25	0.25	0.25	0.25	0.25
Polishing pressure (N)	2.8	2.8	2.8	2.8	2.8	2.8	2.8

Figure 8 shows the polishing results of NPD cutting tools under different rotational speeds. Figure 8 (a) shows the surface roughness of the tool polishing. It is set with a total of seven speeds: 800 RPM, 1000 RPM, 1200 RPM, 1400 RPM, 1600 RPM, 1800RPM and 2000 RPM. As the rotational speed gradually increases, the surface roughness of the cutting edge changes from high to low and then to high.

At a rotational speed of 1600 RPM, the lowest surface roughness is 0.47 nm. Figure 8 (b) shows the blunt radius of the cutting edge, which also shows a trend of decreasing from high to high and then increasing with the increase of rotational speed. When the speed is 1600 RPM, the tool achieves a minimum radius value of 42.16 nm. This indicates that setting the speed to 1600 RPM yields the best polishing effect for the tool.

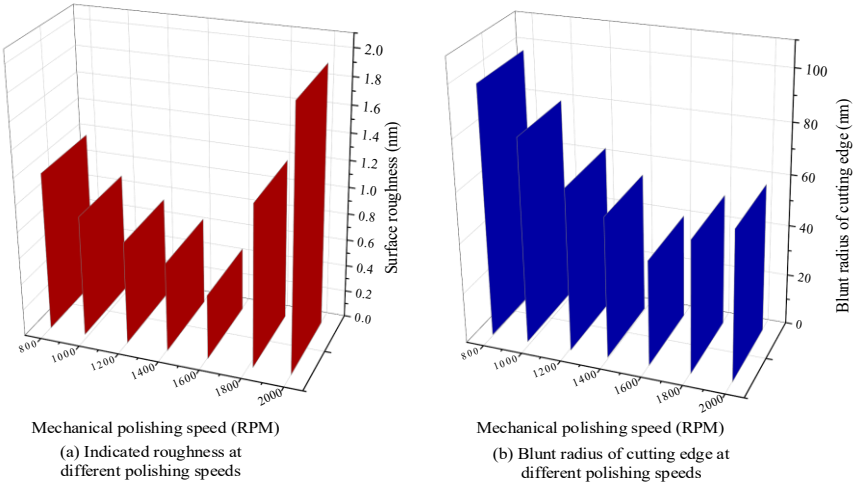

Figure 8: Polishing effect of NPD cutting tools under different speed conditions

3.5 Influence of different Polishing Pressure Conditions on the Polishing Accuracy of Cutting Tools

Next, the rotational speed is kept constant at 1600 RPM, the DAPS is kept constant at 0.25 μm, and different polishing pressure conditions are set for experiments. The different polishing pressure parameter conditions are shown in Table 3. According to the equipment usage requirements, four polishing pressure parameters are set for the experiment, namely 2.6 N, 3.6 N, 4.6 N, and 5.6 N, with the minimum pressure value of the equipment being 2.6 N.

Table 3. Different polishing pressure parameter conditions

Parameter number	1	2	3	4
Disc polishing speed (RPM)	1600	1600	1600	1600
DAPS (μm)	0.25	0.25	0.25	0.25
Polishing pressure (N)	2.6	3.6	4.6	5.6

Figure 9 shows the polishing results under different polishing pressure conditions. Figure 9 (a) shows the surface roughness. As the polishing pressure increases, the surface roughness of the material shows an increasing trend. When the pressure value is 2.6 N, the surface roughness of the tool is 0.45nm. When the pressure is increased to 5.6 N, the surface roughness at this moment is 2.08 nm. The increase in polishing pressure will have a direct impact on the surface roughness of the tool, and the polishing surface roughness of the tool is the smallest at lower pressures. Under high pressure, through microscopic observation, obvious plastic grooves appear on the surface of the cutting tool, and some cutting surfaces even have pits caused by crushing. Next, the effect of the blunt radius under different pressures is analyzed, as shown in Figure 9 (b). As the pressure increases, grooves and pits are formed due to the high pressure, resulting in the phenomenon of detached grains at the edge of the cutting edge, which also leads to an increase in the blunt radius of the cutting edge. When the pressure is set to 2.6 N, the minimum radius value is 40.12 nm. Therefore, the tool polishing effect is optimal when the pressure value is set to 2.6 N.

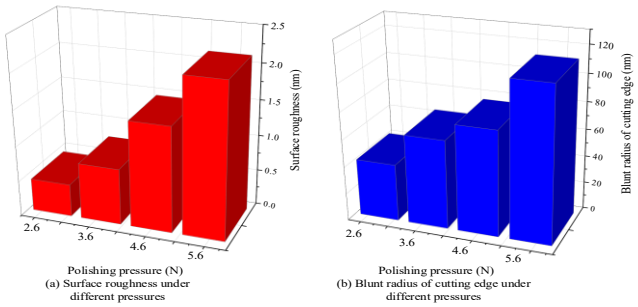

Figure 9: Polishing effect of NPD tool under different polishing pressure conditions

3.6 Influence of Different DAPS Conditions on the Polishing Accuracy of Cutting Tools

The influence of DAPS on the polishing process is further discussed, with a constant pressure of 2.6 N and a constant speed of 1600 RPM.

The specific experimental parameters are shown in Table 4.

DAPS is set to 12 levels, ranging from the lowest 0.25 μm to 6.0 μm, and the equipment can achieve a minimum particle size of 0.25 μm.

Table 4. Parameters of different diamond abrasive particle sizes

Parameter number	Disc polishing speed (RPM)	DAPS (μm)	Polishing pressure (N)
1	1600	0.25	2.6
2	1600	0.5	2.6
3	1600	0.1	2.6
4	1600	1.5	2.6
5	1600	2.0	2.6
6	1600	3.0	2.6
7	1600	3.5	2.6
8	1600	4.0	2.6
9	1600	4.5	2.6
10	1600	5.0	2.6
11	1600	5.5	2.6
12	1600	6.0	2.6

Figure 10 shows the influence of different DAPS on the polishing effect of NPD cutting tools compared based on the above parameters. Figure 10 (a) shows the results of roughness and blade breakage. According to the NPD tool polishing standard, it is required that the edge breakage should be below 0.1 μm. With the continuous increase of DAPS, the surface roughness of the cutting tool and the edge breakage are constantly increasing. The larger the DAPS, the more obvious the surface scratches during the polishing process.

When the particle size is 0.25 μm, the surface roughness and edge chipping are the smallest, at 0.44 nm and 0.36 nm, respectively. Figure 10 (b) shows the result of the blunt radius of the cutting edge. Similarly, the increase in particle size leads to an increase in scratches on the tool surface and affects the cutting edge. When the particle size is 0.25 μm, the minimum cutting edge bluntness radius obtained by tool polishing is 40.11 nm. Therefore, the optimal settings for the NPD tool polishing process parameters, including speed, DAPS, and polishing process pressure, are 1600 RPM, 0.25 μm, and 2.6 N.

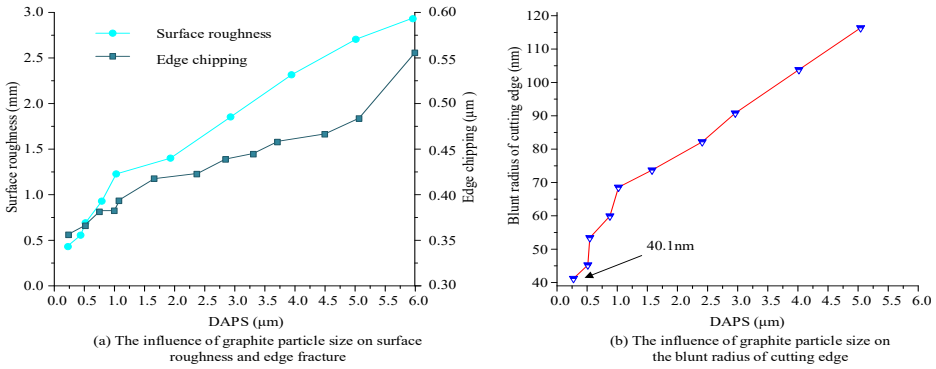

Figure 10: The influence of different DAPS on tool polishing

The optimization of polishing process parameters (speed, pressure, DAPS) is the core part of this study. However, the initial experimental results only provide single-value data and do not verify the reliability of parameter optimization conclusions or the quantitative correlation between parameters and performance indicators. To address this gap, statistical analysis is conducted to enhance the scientific rigor of the research. The average (μ) and standard deviation (SD) of surface roughness and cutting edge passivation radius under various parameter combinations are calculated and Pearson correlation analysis is performed to quantify the linear correlation between various polishing parameters (speed, pressure, abrasive particle size) and two core performance indicators. Finally, multiple linear regression analysis is conducted to establish a regression model between polishing parameters and surface roughness, screen key influencing factors, and verify the optimality of the final determined parameters. The experimental results are shown in Table 5.

Table 5. Statistical results of polishing parameters and core performance indicators (n=5)

Polishing Parameter	Performance Indicator	Pearson Correlation Coefficient (r)	p-value	Standardized Regression Coefficient (β)	Variance Inflation Factor (VIF)
Rotational speed (RPM)	Surface roughness (nm)	-0.89	< 0.001	-0.78	1.05
Cutting edge bluntness radius (nm)		-0.85	< 0.001	-0.72	1.05
Polishing pressure (N)	Surface roughness (nm)	0.94	< 0.001	0.86	1.03
Cutting edge bluntness radius (nm)		0.91	< 0.001	0.81	1.03
DAPS (μm)	Surface roughness (nm)	0.96	< 0.001	0.9	1.04
Cutting edge bluntness radius (nm)		0.93	< 0.001	0.87	1.04
Regression model	Surface roughness (nm)	-	< 0.001	R^2 = 0.95, Adjusted R^2 = 0.94	-

Note: VIF<1.1 indicates no multicollinearity between parameters. The regression equation for surface roughness is: $y = 3.21 - 0.0012x_1 + 0.35x_2 + 0.42x_3$ (x_1 = rotational speed, x_2 = polishing pressure, x_3 = abrasive particle size).

According to the statistical results in Table 5, Pearson correlation analysis shows that the three polishing parameters are extremely significantly correlated with core performance indicators (p<0.001), with DAPS having the strongest positive correlation with surface roughness (r=0.96) and rotational speed showing a strong negative correlation (r=-0.89). The multiple linear regression model has a high fitting degree (R^2=0.95) without multicollinearity (VIF<1.1), and DAPS has the greatest impact on surface roughness (β=0.90). The finally determined parameter combination (1600 RPM, 2.6 N, 0.25 μm) has the best correlation, with an average surface roughness of 0.44 nm (SD=0.02 nm) and an average bluntness radius of 40.11 nm (SD=0.8 nm). The stable data (CV<5%) provides a reliable quantitative basis for process application.

4. Discussion and Conclusion

At present, NPD cutting tools are widely used in the industrial manufacturing field due to their high strength, hardness, and wear resistance, making them an important material in the field of industrial high-precision machining. However, NPD tools are affected by material differences and processing condition parameters during the polishing process. Therefore, this study introduces nanomaterials to improve tool support materials and analyzes the influence of different processing condition parameters on tool polishing.

In the experiment of improving the performance of cutting-edge support, adding 1.25%NAP could increase the hardness of the support material to 1.42 GPa, while 0.2%GNS could increase the hardness to 1.37 GPa. The main reason was that the high specific surface area of NAP formed dispersion strengthening in the Ag-Cu-Ti matrix, and the increase in grain boundary density hindered dislocation movement, significantly improving the material's hardness. In addition, GNS uniformly transferred external loads to the matrix through interfacial shear and suppresses crack propagation through a layered structure, thereby enhancing the fracture toughness of the material. In the impact resistance experiment, when using a content of 1.25%NAP and 0.2%GNS, the stress and ultimate strength of the supporting material reached their maximum values of 7.5 GPa and 4.5 GPa, and the failure stress decreased. In addition, thanks to the synergistic effect of alumina and graphene, the support material reduced the interface height difference from 50.2 nm to 22.2 nm and the blunt radius from 57 nm to 42 nm. The main reason was that alumina improved the interface hardness matching and reduced polishing vibration, while graphene enhanced the interface bonding strength and suppressed the creep deformation of the support material during hot pressing [20].

In the process optimization of NPD cutting tools, the optimal combination of polishing process parameters was obtained when the polishing pressure, speed, and DAPS used were set to 2.6 N, 1600 RPM, and 0.25 μm. Under the polishing process parameters, the surface roughness of the NPD tool was reduced to 0.44 nm, and the bluntness radius was reduced to 40.11 nm. Further analysis revealed that low-pressure (2.6 N) and small abrasive particles (0.25 μm) could effectively control material removal, mainly through plastic deformation, and reduce microcracks caused by brittle fracture. At high speeds (1600 RPM), the frictional heat between abrasive particles and tool surfaces promoted local graphitization, combined with mechanical removal, significantly reducing surface roughness [21].

In summary, this study successfully improves the hardness and impact resistance of the support material by introducing GNS and NAP into the CESM of NPD cutting tools. This provides important technical support for the polishing process of NPD tools and improves the overall effect of subsequent NPD tool polishing processing. This study has certain limitations: only two nanomaterials were used, and the enhancement effect of other materials, such as carbon nanotubes, was not explored. Due to equipment constraints, abrasive particle sizes smaller than 0.25 μm and pressures below 2.6N were not tested. Local agglomeration of nanomaterials may occur in experiments, and a slight temperature rise during high-speed polishing may also affect interface bonding. These uncertainties may lead to minor deviations in results, which need to be improved by expanding material types and optimizing equipment precision in subsequent studies.

Funding

The research is supported by: General Project of Basic Science (Natural Science) Research in Higher Education Institutions of Jiangsu Province: Research on the Preparation of Composites for Tissue Tracheal Stents and Their 3D Bioprinting Molding Process (NO:22KJD460011).

References

[1] Aditharajan A, Radhika N, Saleh B. Recent advances and challenges associated with thin film coatings of cutting tools: a critical review. Transactions of the IMF, 2023, 101(4): 205-221.

[2] Shmatov A A, Soos L, Krajny Z. Application of thermohydrochemical technology of hardening of tools in mechanical engineering. Inorganic Materials: Applied Research, 2023, 14(4): 1052-1058.

[3] Chowdhury M, Kushwah A, Satpute A N. A comprehensive review on potential application of

nanomaterials in the field of agricultural engineering. Journal of Biosystems Engineering, 2023, 48(4): 457-477.

[4] Gupta S, Gupta S, Gupta A. Reimagining Carbon Nanomaterial Analysis: Empowering Transfer Learning and Machine Vision in Scanning Electron Microscopy for High-Fidelity Identification. Materials, 2023, 16(15): 5426-5429.

[5] Ta H T T, Tran N V, Righi M C. Nanotribological Properties of Oxidized Diamond/Silica Interfaces: Insights into the Atomistic Mechanisms of Wear and Friction by Ab Initio Molecular Dynamics Simulations. ACS Applied Nano Materials, 2023, 6(18): 16674-16683.

[6] Zafar S. Biocompatible Nanomaterial TiN, ZrN and TiAlN Thinfilms Coating on Surgical Tools by Cathodic Arc Deposition. Biosensors and Nanotheranostics, 2024, 3(1): 1-10.

[7] Zhang J, Fu Y, Chen X, Shen Z, Zhang J. Investigation of the material removal process in in-situ laser-assisted diamond cutting of reaction-bonded silicon carbide. Journal of the European Ceramic Society, 2023, 43(6): 2354-2365.

[8] Lian Y, Chen X, Zhang T, Liu C,Lin L, Lin F, Li Y. Temperature measurement performance of thin-film thermocouple cutting tool in turning titanium alloy. Ceramics International, 2023, 49(2): 2250-2261.

[9] Cheng Y, Wang Y, Lin J, Xu S, Zhang P. Research status of the influence of machining processes and surface modification technology on the surface integrity of bearing steel materials. The International Journal of Advanced Manufacturing Technology, 2023, 125(7): 2897-2923.

[10] Siddeshkumar N G, Suresh R, Durga Prasad C. Evolution of the surface quality and tool wear in the high speed turning of Al2219/n-B4C/MoS2 Nano metal matrix composites. International Journal of Cast Metals Research, 2024, 37(1): 22-38.

[11] Laghari R A, Jamil M, Laghari A A, Khan AM. A critical review on tool wear mechanism and surface integrity aspects of SiCp/Al MMCs during turning: prospects and challenges. The International Journal of Advanced Manufacturing Technology, 2023, 126(7): 2825-2862.

[12] Pimenov D Y, Kiran M, Khanna N, et al. Review of improvement of machinability and surface integrity in machining on aluminum alloys. The International Journal of Advanced Manufacturing Technology, 2023, 129(11): 4743-4779.

[13] Hamzaban M T, Rostami J, Dahl F, Macias FJ. Wear of cutting tools in hard rock excavation process: A critical review of rock abrasiveness testing methods. Rock Mechanics and Rock Engineering, 2023, 56(3): 1843-1882.

[14] Chen Z, Wu X, Ke W, Shen J, Jiang F, Zhu L. Tool wear mechanisms of PCD micro end mill in machining of additive manufactured titanium alloy. The International Journal of Advanced Manufacturing Technology, 2023, 127(7): 3269-3280.

[15] Zia A W, Anestopoulos I, Panayiotidis M I, Birkett M. Soft diamond-like carbon coatings with superior biocompatibility for medical applications. Ceramics International, 2023, 49(11): 17203-17211.

[16] Adin M Ş. Machining aerospace aluminium alloy with cryo-treated and untreated HSS cutting tools. Advances in Materials and Processing Technologies, 2024, 10(3): 2664-2689.

[17] Ghanim A A J, Amin M, Zeyad A M, Tayeh BA. Effect of modified nano-titanium and fly ash on ultra-high-performance concrete properties. Structural Concrete, 2023, 24(5): 6815-6832.

[18] Zhang C, Vispute R D, Fu K, Ni C. A review of thermal properties of CVD diamond films. Journal of Materials Science, 2023, 58(8): 3485-3507.

[19] Li Q, Yuan S, Gao X, Zhang Z, Chen B, Li Z. Surface and subsurface formation mechanism of SiCp/Al composites under ultrasonic scratching. Ceramics International, 2023, 49(1): 817-833.

[20] Peng Y, Ren J, Jia C, Zhong G, Ma Q, Zhang W. Structural design and mechanical properties of porous structured diamond abrasive tool by selective laser melting. Ceramics International, 2023, 49(4): 6508-6521.

[21] Nengem S M. Symmetric Kernel-Based Approach for Elliptic Partial Differential Equation. Journal of Data Science and Intelligent Systems, 2023, 1(2): 99-104.